INSTITUT DE FRANCE
Académie des sciences

Comptes Rendus

Mécanique

Claude Cambon, Alejandro Alvarez Laguna and Ye Zhou

CFD for turbulence: from fundamentals to geophysics and astrophysics

Volume 350, Special Issue S1 (2022), p. 151-170

Online since: 12 December 2022
Issue date: 5 November 2024

Part of Special Issue: More than a half century of Computational Fluid Dynamics
Guest editor: Mohammed El Ganaoui (Professeur des Universités, Spécialiste : Mécanique des Fluides et Transferts de Chaleur et de Masse, Université de Lorraine)

https://doi.org/10.5802/crmeca.135

CENTRE MERSENNE
The Comptes Rendus. Mécanique *are a member of the Mersenne Center for open scientific publishing*
www.centre-mersenne.org — e-ISSN : 1873-7234

Comptes Rendus
Mécanique
2022, Vol. 350, Special Issue S1, p. 151-170
https://doi.org/10.5802/crmeca.135

Research article / *Article de recherche*

More than a half century of Computational Fluid Dynamics / *Plus d'un demi-siècle de mécanique des fluides numérique*

CFD for turbulence: from fundamentals to geophysics and astrophysics

Claude Cambon [*, a], **Alejandro Alvarez Laguna** [b] **and Ye Zhou** [c]

[a] Laboratoire de Mécanique des Fluides et d'Acoustique, Université de Lyon, UMR 5509, Ecole Centrale de Lyon, CNRS, UCBL, INSA F-69134 Ecully, France

[b] Laboratoire de Physique des Plasmas (LPP), CNRS, Observatoire de Paris, Sorbonne Université, Université Paris Saclay, Ecole polytechnique, Institut Polytechnique de Paris, 91120 Palaiseau, France

[c] Lawrence Livermore National Laboratory, Livermore, California 94550, USA

E-mails: claude.cambon@ec-lyon.fr (C. Cambon), alejandro.alvarez-laguna@lpp.polytechnique.fr (A. Alvarez Laguna), zhou3@llnl.gov (Y. Zhou)

Abstract. Over the years, the combination of computational fluid dynamics (CFD) and theoretical models have critically contributed to improving our understanding of the nature of turbulent flows. In this paper, we review the role of CFD in the study of turbulence through both direct numerical simulations and the resolution of statistical multi-scale theories. With a historical perspective, we will discuss the evolution of the numerical modeling of turbulence from the first numerical experiments as proposed by Orszag and Patterson [1] to complex geophysical and plasma simulations where body forces such as Coriolis, the buoyancy force, or the Lorentz force can introduce strong anisotropies. Looking beyond the horizon, we address the future challenges for CFD and turbulence theorists with the prospect of exascale supercomputing.

Keywords. Turbulence modeling, Direct numerical simulation, Turbulence theories, Statistical closure approaches, Large eddy simulation, Rotating and unstable stratified flows, Plasma and magnetohydrodynamics (MHD) turbulence.

Manuscript received 11 December 2021, accepted 12 September 2022.

1. Introduction

In physics and fluid dynamics, researchers must rely on studies from a combination of theoretical, experimental, and computational approaches. In the domain of fluid turbulence, and beyond (magnetohydrodynamic (MHD), plasmas, environmental multi-physics, etc.), however, computational fluid dynamics (CFD) seems to be increasingly dominant, especially concerning

* Corresponding author

the theoretical component of the trinity. In this article, we hope to relaunch a conversation recently started by the third author [2], on the role of theory, using a review of CFD in fluid dynamics from the sixties to the present. For the sake of conciseness, we will set aside the experimental approach in our essay, even though we are aware of the increasing role of PIV, namely, with a holistic representation of Lagrangian (PTV)/Eulerian fields [3].

As a first point, it is perhaps appropriate to consider CFD and theories as mutually complementary parts of one great scheme. In the best cases, CFD, especially those using a direct numerical simulation (DNS), is a tool for checking theories. Often, at least cross-validation can be performed using CFD for DNS, and CFD for elaborate theoretical models.

This second aspect of CFD, solving equations from statistical multi-scale theories, is often not presented and discussed with enough care in theoretical articles. As a first example, the title of the seminal paper of Orszag about EDQNM closure [4] was "Analytical theories of turbulence", but the spectral closure is of such high complexity that only a numerical procedure allows solving its equations. In this sense, the work by Leith [5] on numerics is essential for exploiting in a quantitative way such a spectral closure. This example concerns only incompressible HIT (Homogeneous Isotropic Turbulence), but the challenge of solving numerically statistical equations is even more difficult when anisotropy is called into play, not to mention compressibility, and/or explicit inhomogeneity. We will illustrate that point with theoretical and numerical studies in anisotropic turbulence subjected to body forces (Coriolis, buoyancy, Lorentz in MHD), from weakly nonlinear (in turbulence, e.g., wave turbulence theory), to strongly nonlinear (e.g., triadic closures).

Of course, we are starting from fundamentals in fluid turbulence, but possible applications to geophysics, astrophysics, and even environmental flow dynamics in multi-physics, cannot be ignored.

Our essay is organized as follows. Section 2 is devoted to the history of DNSs for fundamentals, mainly with pseudo-spectral DNSs in triple-periodic cubic (or parallelepipedic) boxes, from first low resolution, say 32^3 or less, to the recent one, 18432^3 [6]. Section 3 deals with the computational effort to solve quantitatively the closure theories, or elaborate multipoint statistical approaches, to check, cross-validate, with DNSs, before extrapolating them at unprecedented Reynolds numbers and elapsed times. Section 4 will review how fundamental studies of turbulent flows with body forces, Coriolis, and buoyancy, then with mean shear, open the way to geophysical applications. Section 5 will review the applications to astrophysics, or engineering flows for nuclear fusion, with extension to MHD and hot plasmas. In addition to our concluding remarks, the last Section 6 will address the future of CFD, namely for fundamental aspects of fluid and MHD flows. Here, the focus is on the possible role of theory versus CFD (and possibly versus experimental studies, but that subject is beyond the scope of our paper).

2. Pseudo-spectral DNSs in triple-periodic boxes, and beyond

In the last several decades, the power of supercomputers has grown exponentially, presenting new methods to address these challenges. As articulated in [2], the pioneering paper of Orszag and Patterson [1] (see a picture of Professor Orszag in Figure 1) may be the first legitimate "numerical experiment" in fluid dynamics (leaving aside the groundbreaking works of some of the fathers of computational physics such as Ulam [7] and von Neumann [8]). Orszag and Patterson showed that simulations are feasible and even economical at Reynolds numbers of the order achieved in wind-tunnel turbulence experiments at fairly low Reynolds. They also pointed out that the value of the simulations lies not only in the completeness of the data they provide but also in the opportunity they give for the assessment of the accuracy of turbulence theories under controlled and known conditions. The Navier–Stokes equations can be solved numerically with physically consistent accuracy in space and time using DNS (e.g.,

Figure 1. Professor Steven Alan Orszag, *Phys. Today*, with the permission of AIP Publishing. The pioneering paper of Orszag and Patterson [1] demonstrated the power and utility of direct numerical simulation (DNS).

Moin and Mahesh [9]). Despite spanning a wide range of lengths and time scales, the entire flow fields of key idealized flows (e.g., HIT, (Buaria *et al.* [10]; Cao *et al.* [11]; Ishihara *et al.* [12]; Iyer *et al.* [13–15]; Kaneda *et al.* [16]; Yeung *et al.* [17])) can be obtained. Researchers can extract desired information about turbulent structures and statistics by analyzing datasets harvested from the flow fields.

2.1. *Seminal numerical technique*

Starting from the simple case of incompressible homogeneous turbulence, the pseudo-spectral method uses both a grid in physical space and a spectral grid in a cubic box of side L_0 for solving the N–S equations. Wave vectors $\boldsymbol{k}$ are discretized as

$$k_i = k_i^* \frac{2\pi}{L_0}, \quad k_i^* = \pm 1, \pm 2, \ldots \pm N, \tag{1}$$

so that it is generally said that "the box is of side 2π", omitting that a true dimensional length L_0 is implied. Linear terms in N–S equations, first from the viscous term, $\nu\nabla^2 \boldsymbol{u}(\boldsymbol{x}, t)$, becoming local as $\nu k^2 \hat{\boldsymbol{u}}(\boldsymbol{k}, t)$ in 3D Fourier space, are calculated in Fourier space (the "overhat", from now on, denotes the 3D Fourier transform). The nonlinear term, originating from $u_i u_j$ are calculated in physical space, using Fast Fourier Transforms (FFT), direct and inverse, for connecting $\boldsymbol{u}(\boldsymbol{x}, t)$ to $\hat{\boldsymbol{u}}(\boldsymbol{k}, t)$, and reciprocally. Finally, the pressure term is calculated in Fourier space from the projection of the nonlinear term, or $\imath P_{im} k_n \widehat{u_m u_n}$, possibly symmetrised, in order to ensure the divergence-free constraint ($P_{im} = \delta_{im} - k_i k_m / k^2$ is the projection operator).

In a slightly different way, the basic nonlinearity originates from the Lamb vector $\boldsymbol{\omega} \times \boldsymbol{u}$, and passing from vorticity to velocity, and reciprocally, is obvious in Fourier space. In short, the method takes advantage of the local expression of the terms in Fourier space, much simpler than nonlocal Laplacian (dissipation), Poisson (pressure), or Biot–Savart (velocity from vorticity) formulation in physical space; calculation of nonlinear terms in physical space, in turn, avoids the high cost of their calculation as a convolution product is formed in fully 3D Fourier space. The discretization uses $2N$ points per side of the cubic box, so that, e.g., $N = 64$ for a 128^3

DNS. One can recall that a brief order-of-magnitude estimate of the computational task for a full spectral convolution is ($\propto (N^3)^3$) versus the pseudo-spectral (e.g., FFT-based DNS) method of $\propto 3N^3 \log(N)$. The drastic reduction of numerical cost and of the size of memory from the full nonlinear spectral technique to the pseudo-spectral one, cannot be performed without special care and conditions, for instance for avoiding *aliasing* errors. The reader is referred to technical papers for these issues (e.g., see Chapter 9 and Appendix F of the monograph by Pope [18] for more details on pseudo-spectral methods and the FFT technique).

Before discussing other numerical schemes for flows with (more) complex geometry, it is perhaps useful to specify how the use of *Fourier integral transforms* for continuous fields, as a tool for developing statistical theories and models, is different from the approach to periodic flows with discrete fields in pseudo-spectral DNSs. From all the text after the discrete equation (1), only integral forms are used in the following. It is perhaps worthwhile to recall that the same requirements are done for the fluctuating variable in physical space, say $\boldsymbol{u}(\boldsymbol{x},t)$, as its Fourier integral transform $\hat{\boldsymbol{u}}(\boldsymbol{k},t)$, that is expressed in terms of complex numbers, but in a *half-space*, according to the Hermitian property $\hat{\boldsymbol{u}}(\boldsymbol{k}) = \hat{\boldsymbol{u}}^*(-\boldsymbol{k})$. Accordingly, $\boldsymbol{x}$ and $\boldsymbol{k}$ are continuous variables in the domain $[-\infty,\infty]$, or $[0,\infty]$ (half-space), and the case of $|\boldsymbol{k}| = 0$ does exist, in spite of (1). Of course, distributions are used when considering disturbance, possibly stochastic, fields, as $\boldsymbol{u}$ and $\hat{\boldsymbol{u}}$, without need for periodicity, in theories and models, but classical functions are recovered when looking at statistical moments and their spectral tensors. Even in theoretical studies, from DIA and other ones, the ambiguous notation $\sum_{(k=p+q)}$ for the convolution product will be avoided and replaced by an integral formulation. Finally, in terms of motivating FFT-based methods, it might be appropriate to mention that for statistically homogeneous systems, a Fourier representation is typically a *proper orthogonal representation*, perhaps subject to a re-ordering of modes.

Back to flows with complex geometry, the range of scales that needs to be represented in a DNS is determined by the physics. However, the accuracy of this representation is determined by the numerical schemes that are used for the spatial and temporal discretisations. The chosen numerical scheme largely depends on the regime of study (e.g., presence of shocks), the geometry and the set of equations. Some classical numerical schemes used in DNS can be found in the review on compact finite difference schemes, based on Padé approximation, by Lele [19], the monograph on numerical schemes for CFD by Hirsch [20], or on numerical schemes for the MHD equations [21]. Despite the importance of this topic, in this review, we will not tackle extensively issues associated to the numerical resolution of the equations and we refer the interested readers to other works of this special edition.

2.2. *Introduction of effects of body forces, Coriolis, buoyancy, Lorentz*

The principle of pseudo-spectral DNSs is easily extended to flows subjected to body forces, with coupled fields, fluctuating velocity, fluctuating density (or buoyancy within the Boussinesq assumption), fluctuating magnetic field in MHD, in addition to the fluctuating velocity field. The principle of the pseudo-spectral technique remains unchanged, provided that only divergence-free vectorial fields are considered (in the case of incompressible flows). With respect to the basic case of incompressible N–S equations without interactions, new terms ought to be accommodated: the Coriolis force, the buoyancy force, the Lorentz force and their possible combinations. They are related to specific contribution of fluctuating pressure, in order to ensure the divergence-free constraint for vectorial fields, e.g., velocity and magnetic field. Such terms correspond to the solenoidal projection of additional body forces, and are calculated in 3D Fourier space, using the projection operator $P_{im} = \delta_{im} - k_i k_j / k^2$, already used in HIT. Even though the

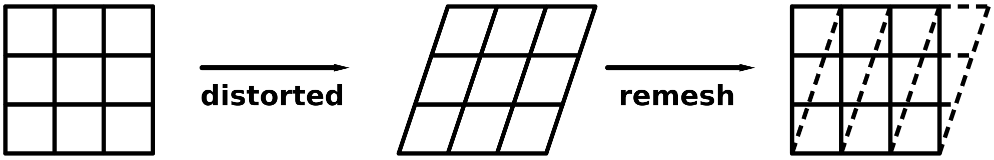

Figure 2. Moving grid for uniform plane shear flow.

numerical technique is easily extended from the seminal technique [1], a new challenge with respect to HIT is the *strong anisotropy*. This implies that statistical spectral quantities are not reduced to, and obtained by, spherical averaging: Extracting from DNS and from the closure equations all the relevant statistics, scale-by-scale and possibly strongly anisotropic, is an important challenge, discussed further.

2.3. *Towards shear-driven flow, from Rogallo [22] to studies in geophysics and astrophysics*

The case of the homogeneous turbulence subjected to a pure plane mean shear displays a more complex additional linear term, that combines both advection and distortion by the mean shear flow. The seminal technique by Rogallo [22] can be easily interpreted as a Lagrangian method reduced to the mean, whereas homogeneity is restricted to the fluctuating flow only. Accordingly, spatial variables in physical space $\boldsymbol{X}$ and in Fourier space $\boldsymbol{K}$ are transformed from the original ones $\boldsymbol{x}$ and $\boldsymbol{k}$ via the following linear mapping

$$x_i = F_{ij}(t,t_0)X_j; \quad k_i = F^{-1}_{ji}(t,t_0)K_j, \tag{2}$$

in which $\boldsymbol{F}$ is the Cauchy matrix derived from the mean velocity gradient A_{ij}, with

$$\dot{F}_{ij} = A_{im}F_{mj}, \quad F_{ij}(t_0,t_0) = \delta_{ij}. \tag{3}$$

The first equation in (2) is related to the mean trajectories; this mapping, with $\boldsymbol{X}$ called Rogallo's space (!) in CTR (Center for Turbulence Research), Stanford, was generalized to linear RDT (Rapid Distortion Theory) by the first author, namely for elliptical flows, and used in DNS by astrophysicists, namely [23] and the "Snoopy" code with new applications. For the sake of brevity, it is sufficient to say that the classical pseudo-spectral method is then applied to "mean-Lagrangian" variables $\boldsymbol{X},\boldsymbol{K}$, or that the original wave vector becomes time-dependent via the second equation in (2). In a recent paper, the convection operator by the mean flow, with space-uniform gradients, is treated by a new scheme, that do not need distortion of the grid and related interpolation (from $\boldsymbol{X}-\boldsymbol{K}$ discretized variables to "Eulerian" ones $\boldsymbol{x}-\boldsymbol{k}$, see Figure 2). In addition to application to a spectral statistical model, by Zhu *et al.* [24], an alternative for DNS (versus Rogallo or Lesur) is in progress.

2.4. *Are such DNS the truth?*

Often DNSs, and sometimes LESs, are considered as the truth, especially with respect to theories and statistical closure approaches. This is not completely true. Even in DNS without explicit "physical" boundaries, the relevance of a DNS partly depends on the building of the field for initializing it, e.g., for time history, or on the process to force it, in the case of forced turbulence. Narrowband (in Fourier space) stochastic forcing is artificial and often unphysical, especially at a large scale (or low wavenumber). Coupled with the sparse discretization at low wavenumber, in conventional pseudo-spectral DNS, the forcing yields to scrambling and loss of accuracy in the largest scales, e.g., for non-dimensional wavenumbers k^* from 1 to 10, even at the highest overall resolution. Often, this does not cause a problem for the results in forced HIT, but it could be an issue in anisotropic flows, e.g., rotating flows, in which the mechanisms of building anisotropy are very subtle. Extraction of accurate statistics, both multi-scale and anisotropic is another difficulty. For instance, in unforced turbulence spatial averaging ought to be used by assuming some ergodicity (unlike the forced case where time averaging is possible). Another example is the spherically-averaged energy spectrum in anisotropic DNS where some difficulties appear to compare with results from elaborate theories or closures spectrum when computing the anisotropic spectrum as $\mathscr{E}(k_\perp, k_\parallel, t)$, with $\mathscr{E}(k,t) = E(k)/(4\pi k^2)$. Of course, ensemble average, using several realizations of the basic fields are never used in DNS, given the cost and the very slow convergence of statistics. When it is written that initial data are "turbulent", this means that the initial field is built with a choice of random phases, but this choice is given once for all, and eventually, a single realization of the field is calculated anyway. The increase in the computational resources may allow for using actual ensemble averages in the future [25]. Another limitation of DNSs is the Reynolds number, even with rapid progress, according to the Moore's law, and the future promise of the exascale resolution.

What is a sufficiently large Reynolds number, or another non-dimensional parameter, depends on the physical case under consideration. Based on a study of interacting scales, Ref. [26] identifies the lowest Reynolds number that must be obtained by DNS or experiment to capture all of the significant dynamic scales, a minimum Reynolds number of $\sim 1.6\times 10^5$ or Taylor-based Reynolds number of Re_λ of ~ 1000. Several major computational and experimental studies are consistent with this criterion, where the values of Reynolds number are (i) 3×10^8 (out-scale Reynolds) for the tidal channel [27]; (ii) $Re_\lambda \sim 1300$ from the DNS by Yeung and Ravikumar [6]; (iii) $Re_\lambda \sim 3.2\times 10^3$ (return channel) or 2×10^3 (mixing layer) from very large wind tunnel experiments by Praskovsky *et al.* [28] (iv) $Re_\lambda \sim 1450$ from another very large wind tunnel experiment by Saddoughi and Veeravalli [29]. Using several experimental and simulation datasets, Figure 4.6 of [30] shows that $Re_\lambda > 5\times 10^3$ is sufficient for forced turbulence to recover the Kolmogorov 4/5 law. However, this figure also indicates that an order of magnitude higher Re_λ is needed for decaying turbulence, which might be sensitive to initial conditions, to approach the 4/5 scaling.

Other examples are the Nusselt–Rayleigh law for thermal convection, with a Rayleigh number of 10^{13} (see [31] and references therein). Simpler flows, as basic MHD in liquid metals, call into play a magnetic Prandtl number as low as 10^{-6}–10^{-8}. Finally, we will consider the case of unstably stratified turbulence, in which unprecedented calculations were carried out using both DNSs and anisotropic triadic statistical closures (see Section 3.2), with a major contribution from scientists of the CEA (French Center for Atomic Research).

3. CFD for solving multiscale, or spectral, statistical equations, in theories and closures

3.1. *Essentials of the Leith computational model for triadic closures*

Let us start with the Lin equation, for the spherically integrated energy spectrum $E(k,t)$

$$\left(\frac{\partial}{\partial t} + 2\nu k^2\right) E(k,t) = T(k,t).$$

Of course, this equation presents interest if the right-hand-side term, or transfer term T, is correctly evaluated. All elaborate triadic closures respect the structure of this term as a 3D integral in Fourier space, from the triple correlations at three-points, whose spectral counterpart calls into play all the triads $\boldsymbol{k}+\boldsymbol{p}+\boldsymbol{q}=0$, or

$$T(k,t) = \int\int\int_{R^3} S(k,\boldsymbol{p},\boldsymbol{q})\,\mathrm{d}^3\boldsymbol{p},$$

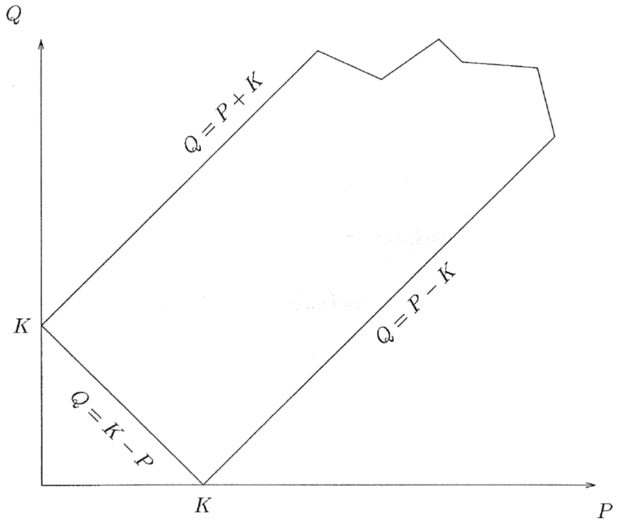

Figure 3. Domain Δ_K for P and Q modulus at fixed K.

where $S(\boldsymbol{k},\boldsymbol{p},\boldsymbol{q})$ is related to the triple correlation by

$$S(\boldsymbol{k},\boldsymbol{p},\boldsymbol{q}) \;=\; \frac{\imath}{2}P_{imn}(\boldsymbol{k})\overline{u_m(\boldsymbol{q})u_n(\boldsymbol{q})u_i(\boldsymbol{k})}$$
$$\text{with } P_{imn}=\frac{1}{2}(k_m P_{in}(\boldsymbol{k})+k_n P_{im}(\boldsymbol{k})) \quad \text{and} \quad P_{ij}=\delta_{ij}-\frac{k_i k_j}{k^2}. \tag{4}$$

This integral can be simplified, e.g., for accommodating 3D isotropy. For this purpose, the set of integrating variables in Cartesian coordinates (p_1,p_2,p_3) is replaced by a bipolar system, or (p,q,λ), so that

$$\int\int\int_{R^3} S(\boldsymbol{k},\boldsymbol{p},\boldsymbol{q})\,\mathrm{d}^3\boldsymbol{p}=\int_0^{2\pi}\left[\int\int_{\Delta_k} S(\boldsymbol{k},p,q,\lambda)\frac{pq}{k}\,\mathrm{d}p\,\mathrm{d}q\right]\mathrm{d}\lambda, \tag{5}$$

and finally, thanks to isotropy,

$$T(k)=2\pi\int\int_{\Delta_k} S(k,p,q)\frac{pq}{k}\,\mathrm{d}p\,\mathrm{d}q. \tag{6}$$

In the bipolar representation, p and q at fixed k are in the domain Δ_k (on Figure 3) for the triangle whose sides have length k, p and q, whereas λ refers to the angle of the plane of the triad rotating around $\boldsymbol{k}$. $(pq)/k$ is the Jacobian of the bipolar transform. In the EDQNM closure for HIT, $S(k,p,q)$ is proportional to $\mathscr{E}(q,t)(\mathscr{E}(p,t)-\mathscr{E}(k,t))$, with $\mathscr{E}(k,t)=E(k)/(4\pi k^2)$. The wavenumbers in E are discretized according to a logarithmic step, with $\Delta k_n/k_n=$ Constant, so that $T(k_n)$ is expressed by a very simple discrete summation. This technique allows ensuring a zero value to the integral $\int_0^\infty T(k,t)\,\mathrm{d}k$ with the highest numerical accuracy. The latter property corresponds to the detailed conservation of energy by triads in 3D. Because Leith addressed 2D HIT as well, it is perhaps useful to recall that the structure of (6) is only modified by a different Jacobian and that both $\int_0^\infty T(k,t)\,\mathrm{d}k=0$ and $\int_0^\infty k^2 T(k,t)\,\mathrm{d}k=0$, ensuring the detailed conservation of both energy and enstrophy.

3.2. *Towards "weak" (nonlinear) wave turbulence theory and strong turbulence*

Two examples are considered as follows, yielding some success stories, rotating turbulence and unstably stratified turbulence. The case of a purely rotating flow seems to be very simple, there is no distortion, and thereby no direct production of energy by the Coriolis force. But the interplay of linear and nonlinear terms is very subtle. Helical modes can be used instead of the Cartesian coordinates for $\hat{\boldsymbol{u}}$. Helical modes [32], introduced as $\boldsymbol{N}(\pm\boldsymbol{k})$ in [33], are eigenmodes of the Curl operator, as $\boldsymbol{N}(\pm\boldsymbol{k})\exp(\pm\imath\boldsymbol{k}\cdot\boldsymbol{x})$. They simplify the basic equations, even without basic rotation, from the expression of the Lamb vector in 3D Fourier space $\widehat{\boldsymbol{\omega}\times\boldsymbol{u}}$, and allow to ensure the solenoidal constraint ($\nabla\cdot\boldsymbol{u}=0, \boldsymbol{k}\cdot\hat{\boldsymbol{u}}=0$), in avoiding *the byzantine use of projectors* (from Leaf Turner, Los Alamos). In addition, they diagonalize the operator of inertial waves in a rotating frame. The helical decomposition can be written

$$\hat{\boldsymbol{u}}(\boldsymbol{k},t)=\sum_{s=\pm1}u_s(\boldsymbol{k},t)\boldsymbol{N}(s\boldsymbol{k}), \tag{7}$$

for the velocity fluctuation. Triadic closures, as the theory of inertial wave turbulence, deal with second-order and third-order correlations. The second-order spectral tensor is the spectral counterpart of two-point second-order velocity correlations. From (7), it is projected on $N_i(\pm\boldsymbol{k})N_j(\pm\boldsymbol{k})$ and can be expressed with the reduced set ($\mathscr{E}, Z, \mathscr{H}$), or energy spectrum, polarization anisotropy (Z is complex-valued) and helicity spectrum. In the presence of system rotation, the equations for ($\mathscr{E}, Z, \mathscr{H}$) are decoupled for their linear part and call into play generalized transfer terms mediated by three-point third-order correlations. The structure of these transfer terms is given by (5), in which $S_{ijm}(\boldsymbol{k},\boldsymbol{p},\boldsymbol{q},t)$ is projected on $N_i(s_k\boldsymbol{k})N_j(s_p\boldsymbol{p})N_m(s_q\boldsymbol{q})$, with $s_k, s_p, s_q=\pm1$, again from (7). A conventional, but *anisotropic*, Lin equation is recovered for the energy as

$$\left(\frac{\partial}{\partial t}+2\nu k^2\right)\mathscr{E}(\boldsymbol{k},t)=\mathscr{T}(\boldsymbol{k},t), \tag{8}$$

with similar equations for the helicity spectrum and the polarization anisotropy Z, or more precisely, its slow part excluding the rapid phase shift of inertial waves, or $Z(\boldsymbol{k},t)\exp(4\imath\sigma_k t)$, where

$$\sigma_k=2\boldsymbol{\Omega}\cdot\boldsymbol{k}/k=2\Omega\frac{k_\parallel}{k}=2\Omega\cos(\boldsymbol{k},\boldsymbol{\Omega}) \tag{9}$$

is the (linear) dispersion frequency of inertial waves in the rotating frame, with angular velocity $\boldsymbol{\Omega}$. The numerical solution for (9) is much more difficult and complex than in HIT, because of the anisotropic structure of its right-hand side. In the asymptotic limit of inertial wave turbulence theory, at vanishing Rossby number and infinite Reynolds number, the nonlinearity is reduced to resonant triads in $\mathscr{T}(\boldsymbol{k},t)$. In the AQNM (Asymptotic quasi-normal Markovian) model [34], the calculation of the generalized transfer term is accurately performed in the close vicinity of the surfaces given by the resonance condition $k_\parallel/k\pm p_\parallel/p\pm q_\parallel/q$, in the full 3D domain of p, q, λ variables in (5) at fixed $k, k_\parallel/k$. For numerical convenience, however, a finite value of ν is kept in (8). This procedure allows deriving many more results on the whole spectral domain than the analytical study of Galtier [35]), which is restricted to a thin band of $k_\parallel/k$ (tending to 0 with the Rossby number) and excludes the exact 2D limit $k_\parallel=0$. It is possible to match the asymptotic AQNM model to the EDQNM3 one, valid for finite Rossby and Reynolds numbers, through a classical eddy damping, that vanishes in the asymptotic limit. Recent DNS and theoretical studies were carried out at IRPHE to study the stability of the geostrophic mode, as in [36].

Unstably stratified homogeneous turbulence (USHT) is another case, using high-resolution CFD for both DNSs and anisotropic triadic closure with unprecedented resolution. The USHT is closely related to Rayleigh–Taylor and Richtmyer–Meshkov instability induced flows [37, 38], which plays a significant role in inertial confinement fusion implosions, supernovae explosions, and many other important applications [39, 40].

Extrapolation of the results of high-resolution DNSs can be carried out by multimodal anisotropic EDQNM until huge Reynolds numbers, and huge elapsed times, after the cross-validation DNS/EDQNM at the highest resolution permitted by DNS. A typical result obtained by the EDQNM model is the scale-by-scale distribution of anisotropy, which is expected to vanish for length scales smaller than an Ozmidov one, or $L_N = \sqrt{\varepsilon/N^3}$, where N is the stratification frequency and ε the dissipation rate. It is shown that isotropy is recovered for anisotropic spectra, at wavenumbers larger than $1/L_N$, for the potential energy at $Re = 10^6$, but not for the kinetic energy, whose re-isotropization needs an ever-larger Reynolds number (Figure 10.23 in [30]).

Another result concerns the infrared range, or the domain of very low wavenumbers, where the resolution of DNS, and especially its anisotropic description, is very sparse (see Section 2.4). In this domain, the multimodal anisotropic EDQNM model reduces to viscous linear dynamics (RDT), where the effective diffusion effect is mediated by a spectral backscatter from the smallest scales. Theoretical predictions are derived for the slopes of the spectra in the infrared range, depending on the initial data. More generally, these results suggest complementing DNS by a theoretical *Supergrid Scale model* (See Soulard *et al.* [41] and reference therein).

More conventional, with Subgrid Scale (SGS) models, an extension of pseudo-spectral DNS to LES in the hydro case is touched upon in conclusion, whereas this topic is addressed in Section 5.2 in the magnetized case.

4. CFD towards geophysical applications

A larger part of this review will address the case of magnetized fields, in the next section. This topic is relevant for geophysics only in the upper atmosphere, or magnetosphere, and in the liquid metal core of the Earth, but we will first consider applications to atmospheric and oceanic flows, in three parts, as follows.

(i) DNS, LES, and spectral statistical closures are relevant for our basic knowledge of rotating and stably stratified flows. It is important to distinguish the cases with and without forcing. The first case in rotating flows roughly recovers that energy concentrates on the 2D modes, as suggested by the Proudman theorem; in this case, the important Coriolis parameter should be less the Rossby number than a kind of Rayleigh number, the ratio of the external force to the Coriolis force. In the unforced case, however, the interplay of (nonlinear) inertial waves with the QG mode is much more subtle, see again [36], and a complex anisotropy can be analyzed scale-by-scale, up to the largest, as in Delache *et al.* [42]. Among several studies carried out by the team of Annick Pouquet, the analysis of the strength of the inverse cascade in rotating stably-stratified flows is performed for a large range of the N/f (stratification to Coriolis frequency) parameter (see Marino *et al.* [43], Figure 11.5). As for the interpretation of Nastrom–Gage spectra, the scalings in terms of N and f were recently revisited by Galperin and Sukorianski [44], with the new observation that these scalings are latitude-dependent. Local structure with scalings of atmospheric or oceanic turbulence can be investigated using the additional S, shear rate parameter (see Chapter 11 in [30] on "N, S, f" couplings), with baroclinic and precessional effects, namely. Finally, at the largest scale, atmospheric and oceanic flows, and even plasmas in the next section, are often dominated by zonal jets, which are investigated in the recent book edited by Galperin and Read [45].

(ii) It is possible to move from small scale and mesoscale to synoptic scales, towards global planetary circulation. Planetary circulation mainly results from the combination of a meridional motion with a zonal one. The meridional convective motion is induced by the differential solar heating, from cold polar zones to the hot equatorial belt. The trends to create zonal flows is then induced by the Coriolis force. Planetary circulation is dominated by zonal jet flows in the atmosphere of giant planets, and the circulation is rather stable and predictable. Even the red spot of Jupiter can be observed almost unchanged from observations separated by decades! The situation is much more complicated, more chaotic and less predictable in our Earth, because of its size and its rotation rate, both moderate. Of course, an additional difference is the inner

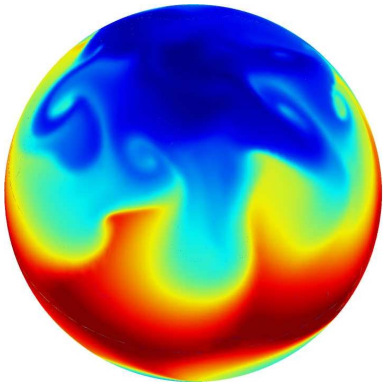

Figure 4. Global atmospheric model simulation with a quadtree-adaptive mesh algorithm. The model solves for a general circulation model and, in the figure, we show a snapshot of the temperature. The finest mesh resolution is of the order of 1° of the sphere (i.e., ∼100 km in the equator, which would allow for capturing a cyclone event). (Courtesy of S. Popinet).

structure of giant planets versus rocky ones. In spite of the high complexity of the dynamics of Earth's atmosphere, simple models are very efficient, at least for short-time prediction or forecast. In a quasi 2D geostrophic model, isobar lines are streamlines, and it is possible to derive many useful information from a classical map of isobars, about cyclonic and anticyclonic winds, and so on. An unexpensive computational approach is derived with close connection to the *Resolvent analysis* (RA) carried out for near-wall turbulence (e.g., McKeon [46]) and geophysics (e.g., Farrell *et al.* [47]). The dynamical approach combines a linear action of a mean flow on a fluctuating one, with a feed-back from the fluctuating to the mean via (gradients of) the generalized Reynolds stresses. As in RDT, the interaction of the fluctuating flow with itself is ignored; in this sense the so-called *adiabatic reduction* is similar to RA and RDT; for the quasi-2D planetary circulation the mean flow is obtained by zonal averaging and only depends on the latitude.

(iii) Finally, we can say a few words of CFD for environmental flows, with various approaches, from RANS to DNSs, with many hybrid methods. In atmospheric and oceanic models, the massive disparity between the largest and the smallest eddies requires the use of subgrid models. Since the first atmospheric climate models [48], it was realized that the parameterization of the subgrid interactions impacts the accuracy of the large-scale flows. This effect is even more complicated in oceanic climate models as baroclinic instability occurs at much smaller scales. Statistical dynamical closures are also used for determining SGS models in oceanic and atmospheric simulations. Frederiksen and co-workers developed eddy damped quasi-normal Markovian (EDQNM) and DIA closure models for barotropic turbulent flows in spherical geometry, including a quasi-diagonal DIA (QDIA) closure for inhomogeneous turbulence.

Despite the theoretical efforts, the closure models are difficult to be applied into multi-field models such as General Circulation Models (GCMs). For this reason, a direct stochastic modelling approach may be a more tractable methodology as well as entropy approaches as proposed by Holloway [49].

Alternatively, RANS approaches are also used in multi-field atmospheric GCMs models that can be solved with mesh adaptation as proposed by van Hooft *et al.* [50]. An example of the GCM with adaptive mesh is shown in Figure 4. Similarly, for ocean GCMs, RANS models are used such as the one proposed by Gent and McWilliams [51], which mimics the effects of baroclinic turbulence.

Adequate treatments of turbulence will become increasingly prominent for the design of nextgeneration climate models. One example of this is the study by Williams [52] and Watanabe *et al.* [53] that predict that the amount of clear air turbulence will increase significantly in the future as the climate changes on transatlantic flight routes and over the North Pacific. Similarly, due to the uncertainty associated with the clouds' response to warming, future atmosphere models require high-resolution simulations (with adaptive mesh refinement of Figure 4). The interested reader in the physics of climate variability and climate change is referred to Ghil and Lucarini [54]. Furthermore, Pressel *et al.* [55] also discussed the utility of explicit and implicit subgrid models in large eddy simulations of stratocumulus clouds.

5. CFD towards astrophysics, MHD and plasmas

The theories and numerical techniques for hydrodynamic turbulence that we have reviewed above have been applied and extended to plasmas (ionized matter composed by ions and free electrons). However, as we will review below, plasma turbulence have particularities due to their interplay with the electromagnetic field. In this section, we will review the history of DNSs in MHD as well as some statistical closures and SGS/LES models. Finally, we will discuss some applications for astrophysical and laboratory plasmas. The task of doing a complete review is daunting. For this reason, we refer the interested readers to the excellent monographs in the references [56–58], Chapter 12 of [30], and Section 11 of [2] for more details.

5.1. *Main differences between plasma and hydrodynamic turbulence*

The first particularity of plasmas, especially in astrophysical scenarios, is the large-scale separation between the problem size, the ion scales, the electron scales, and the dissipation scales. This separation of scales is shown by Kiyani *et al.* [59] as measured *in situ* in the solar wind. These measurements show different inertial ranges in the energy spectrum, one at scales larger than the gyroradius and another one for scales below the gyroradius. Despite the challenge of describing all these scales, most of the work focuses on the evolution of the macroscopic and the scales larger than the ion gyroradius, as described by the MHD equations.

The second difference from the hydrodynamic turbulence is that the MHD turbulent fluctuations are accompanied by magnetic field motions. In the presence of a large-scale magnetic field $\mathbf{B}_0$, the *Alfvénic* perturbations produce fluctuations of the velocity and magnetic field transverse to $\mathbf{B}_0$ that propagate at the Alfvén speed $v_A = B_0/\sqrt{4\pi\rho_0}$ along $\mathbf{B}_0$. These perturbations can be described by a reduction of the MHD equations that solve for the so-called Elsässer fields, $\mathbf{Z}^{\pm} = \mathbf{u} \pm \mathbf{b}/\sqrt{4\pi\rho_0}$, where $\mathbf{u}$ and $\mathbf{b}$ are the fluid and magnetic-field perturbation perpendicular to $\mathbf{B}_0$; $\mathbf{Z}^{+}$ propagates along $\mathbf{B}_0$ and $\mathbf{Z}^{-}$ in the opposite direction.

The presence of a large-scale magnetic field $\mathbf{B}_0$ cannot be eliminated by a Galilean transformation and hence it introduces a different time scale associated to the Alfvén speed. This scale can therefore change the energy-transfer time across the inertial range. By using this time instead of the eddy-turnover time, Iroshnikov (1963, in [2]) and Kraichnan (1965c, in [2]) proposed a different energy spectrum that in MHD turbulence has a slope at $-3/2$ instead of the $-5/3$ of the "Kolmogorovian" vision. However, both the Kolmogorov and the Iroshnikov–Kraichnan spectra assume the turbulence to be isotropic. In the presence of a magnetic field, as the magnetic field resists bending, the small-scale modes are primarily excited perpendicular to the magnetic field, $k_\perp \gg k_\parallel$. This anisotropy was taken into account by Goldreich and Sridhar [60] to derive a different phenomenological cascade, which in the case of strong turbulence (critical balance) evolves as a Kolmogorov cascade in the perpendicular direction and as a $-5/2$ cascade parallel to $\mathbf{B}_0$. As we will see in the following, the slope of the inertial range in MHD is still an open question that illustrates the difficulty of plasma turbulence.

Plasma turbulence has an additional difficulty due to the many different regimes that can arise, e.g., the presence or not of a large-scale magnetic field (isotropic/anisotropic turbulence), different dissipation regimes (i.e., regimes of kinetic Reynolds and magnetic Reynolds), balanced/imbalanced turbulence (i.e., zero/non-zero cross-helicity), weak/strong turbulence, MHD/Hall-MHD turbulence (i.e., turbulence in scales larger or smaller than the ion gyro-radius), different partition between kinetic and magnetic energies, etc.

In addition, MHD turbulence is more "intermittent" than hydrodynamic turbulence. The intermittency in plasmas is also linked to the self-organization into elongated current sheets (structures with electrical current confined into a high aspect ratio regions). The link between turbulence and magnetic reconnection and the tearing mode (the condensation of the current inside the sheet into magnetic islands) is still an open question in plasma turbulence and numerical simulations can play an important role to unveil the influence of the local reconnection in the global dynamics.

5.2. *From fundamental DNS to statistical closures and LES modelling*

The first DNS simulations of MHD turbulence appeared in the late 70s in the wake of the work on hydrodynamic turbulence. The work of Montgomery and co-workers [61], Pouquet and Patterson [62] or Orszag and Tang [63] paved the way by addressing fundamental questions on the inertial-range cascade, turbulent dynamo or intermittency. However, the Reynolds numbers and resolutions that could be achieved at the time (e.g., $R_\lambda \sim 40$, 32^3 points of Pouquet and Patterson [62]) did not allow to clearly distinguish the slope of the cascade. By the end of the subsequent decade, the improvement in the computational performance, allowed for higher resolutions and Reynold numbers, e.g., $R_\lambda \sim 160$ and 1024^2 by Biskamp and Welter [64]. Nevertheless, in the 90s, the question about the spectral indices of the cascade was still in the spotlight due to the limitation of the simulations, e.g., 180^3 points and $R_\lambda = 544$ by Politano *et al.* [65]. The first works that showed high-resolution 3D simulations appeared in the beginning of the new century [66] with simulations with 512^3 nodes and $R_\lambda \sim 100$), which found that the spectrum in 3D was showing a Kolmogorov-like spectrum. However, the better-resolved 3D simulations of the beginning of the century did not fully address the questions on the paradigm for the MHD turbulent cascade. Mininni and Pouquet [67] presented a numerical analysis of 3D incompressible free-decaying MHD turbulence run on a grid of 1536^3 points and $R_\lambda \sim 1100$, with an energy spectrum that is a combination of two components: at small scales, it shows a k^{-2} spectrum whereas at the large scales, a law compatible with the $k^{-3/2}$ Iroshnikov–Kraichnan theory. In order to shed some light in this apparent discrepancy between the numerical results and the different scaling laws, a novel idea came to the scene: the dynamic alignment by Boldyrev [68]. This theory could explain the $k^{-3/2}$ energy spectrum with ideas that were compatible with [60] model. However, this theory was contested by Beresnyak [69] who claimed that the theory failed at small scales. This history of the evolution of paradigm in MHD turbulence brings us to our days. The best-resolved numerical simulations can be found in [70] with 4096^3 points and $R_\lambda \sim 2000$, supporting a $-5/3$ law. Other recent work that illustrates the state-of-the-art in DNS MHD turbulence are Linkmann *et al.* [71] and Bandyopadhyay *et al.* [72] with magnetic Prandtl numbers different to unity MHD with a strong magnetic field at a resolution of 2048^3, or on elongated periodic domains with $16384 - 2048^2$ grids [73, 74].

Complementary to DNS, CFD is also used to solve statistical closures for MHD turbulence. In plasma turbulence, the "weak" wave turbulence theory [75–77] takes a significant body of the literature. Nevertheless, as discussed by Zhou [2], Cambon *et al.* [78], Sagaut and Cambon [30], this theory is connected to QNM models. In isotropic EDQNM models, the seminal work of

Pouquet *et al.* [79] found a new eddy-damping with the contribution of three terms: the non-linear eddy-distortion rate, the non-local effect determined by the field (effect of Alfvén waves), and the collisional dissipation effects. Matthaeus and Zhou [80] generalized the triple correlation decay time from previously presented "golden rules" as proposed by Grappin *et al.* [81, 82] for correlated turbulence and Pouquet *et al.* [79] for helical turbulence. More recently, Briard and Gomez [83] reexamined the EDQNM for decaying isotropic, homogeneous MHD, showing the impact of the cross-helicity on the global dynamics. Several models have attempted to include anisotropy into the EDQNM closure. In the low-magnetic Reynolds regime (also called quasi-static MHD) Cambon [84] proposed the first *strongly* anisotropic EDQNM approach that was revisited and investigated by Favier *et al.* [85] by taking into account the EDQNM1 and EQNM2 models (see Sagaut and Cambon [30]). Zhou and Mattheus [86] have generalized the eddy-damping relaxation time by taking into account the anisotropic feature in the Alfvénic time, as previously discussed by Goldreich and Sridhar [60], Ng and Battacharjee [87], Galtier *et al.* [77].

As we have seen above, the interaction between the large and the small scales plays an important role in MHD turbulence, which can impact LES/SGS modeling [88]. SGS models for MHD turbulence have been mostly constructed as extensions of the nonmagnetized hydrodynamic models. Some examples of MHD gradient-diffusion-type SGS models can be found in Agullo *et al.* [89] and Müller and Carati [90] for magnetic Prandtl unity or Knaepen and Moin [91] for small magnetic Prandtl number. A Smagorinsky-type SGS model was proposed by Yoshizawa [92] motivated by statistical results from a multi-scale DIA formulation. Spectral eddy viscosity and resistivity, and backscatter viscosity and resistivity were computed using the EDQNM simulations by Zhou *et al.* [93]. A coarse-graining methodology was used by Aluie [94] to derive effective equations for the subscale stress and a subscale electromotive force. Additionally, technique of the renormalization group theory was also proposed for the MHD equations as reviewed by Zhou [95].

5.3. *Towards more complex DNS, LES for plasmas, from laboratory to stars*

The turbulence theories and models described above have offered a fundamental support to the simulations of astrophysical and laboratory plasma phenomena. Carrying out a systematic review of all these applications is colossal and, therefore, we will limit our review to some representative examples. We will start with the models describing the cyclic regeneration of the Sun's large-scale magnetic field, which is at the origin of the "solar activity" [96, 97]. The solar cycle is captured by the anelastic incompressible MHD equations (see e.g., Lantz and Fan [98] and Braginsky and Roberts [99]) that simulate the convective zone of the Sun (the computational domain represents a shell that extends from around 0.72 to 0.97 of the solar radius): a rotating ($Ro < 1$) and unstably stratified thermally-driven turbulent convective plasma (with $Re > 10^{10}$ and $P_m < 10^{-3}$). The turbulent motion produces a mean electromotive force due to the fluctuation of the flow and the magnetic field that is usually modelled with an ILES technique [100] or prescribed SGS coefficients [101]. More complex models are used to simulate smaller portions of the convective zone (see e.g., Figure 5 and Kitiashvili *et al.* [102], Wray *et al.* [103]) through the compressible MHD equations coupled to the radiative transfer equation. In these simulations, LES SGS turbulence models are used, inspired by the hydrodynamic models by Smagorinsky [48] and Moin *et al.* [104].

Above the convection zone lies the solar atmosphere, a complex layer of plasma that extends from the weakly-ionized collisionally dominated photosphere to the fully-ionized magnetically-dominated corona. The transition between these layers, the so-called chromosphere, is a very dynamic region where the motion of the neutral gas and the plasma decouples and therefore the non-equilibrium effects are fundamental to explain the dynamics (see, Alvarez Laguna *et*

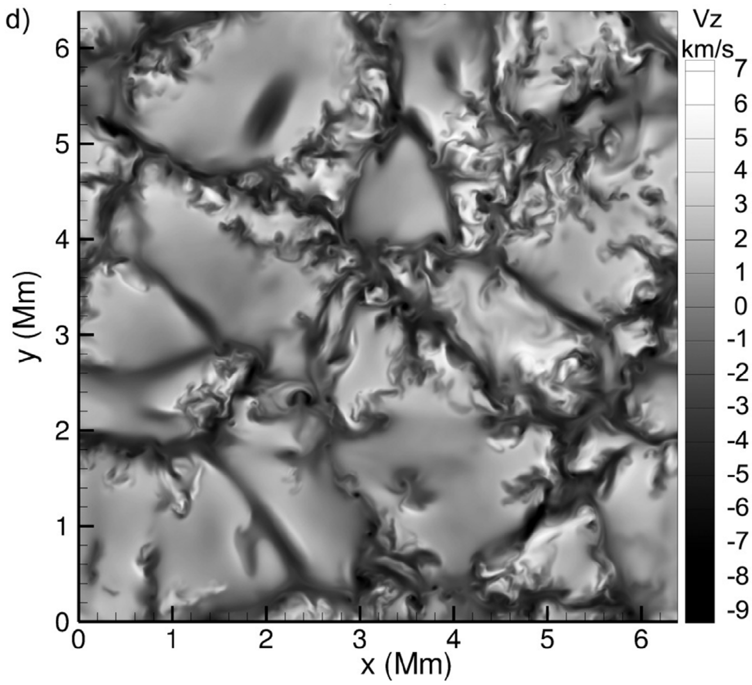

Figure 5. Vertical velocity at the solar photosphere in a solar granulation simulation from the Stellar box code [103]. The simulation combines the MHD equations with an LES model to the radiative transport equation. The resolution is 12.5 km.

al. [105]). In particular, the magnetic reconnection is invoked to play a fundamental role in heating the atmosphere to the 10^6 K of the corona (see Alvarez Laguna *et al.* [106]). Numerical simulations of small regions of the lower sun atmosphere combine the MHD equations (in some cases the multi-fluid equations to model the neutral gas dynamics) with radiation models and non-equilibrium models (Khomenko *et al.* [107], Maneva *et al.* [108], Gudiksen *et al.* [109], Kitiashvili *et al.* [110]). Due to the complexity of the simulations (shocks, magnetic reconnection, non-equilibrium effects), the role of turbulence is still an open question in these simulations.

The outer layer of the sun, the solar corona stretches out into the heliosphere by means of the solar wind. Van de Holst *et al.* [111] proposed a global model from the upper chromosphere to the corona and the heliosphere that takes into account the Alfvén wave turbulence (as previously proposed by Dmitruk *et al.* [112]) by resolving an equation for the wave energy density for the two Elsässer variables.

Another scenario of interest for plasma physicists are the astrophysical disks. These disk accrete thanks to the turbulent transport of angular momentum that is larger than the collisional one. The model of a Taylor–Couette flow with an inner radius and an outer radius, and centered on the center of the star (or the presumed black hole) is very popular. But the most radical simplification was proposed by Balbus and Hawley [113], as the Shearing Sheet Approximation (SSA) sketched on Figure 6.

However, a non-local effect that participates in the inverse energy cascade and which is not captured by local averaging schemes is vortex merger. This conclusion was shown by Salhi and Cambon [114], comparing rapid distortion theory to DNS and LES.

Finally, we will briefly discuss turbulence scenarios in laboratory plasma simulations. Anomalous transport plays a fundamental role in fusion plasmas (see e.g., Balescu [115]), as well as

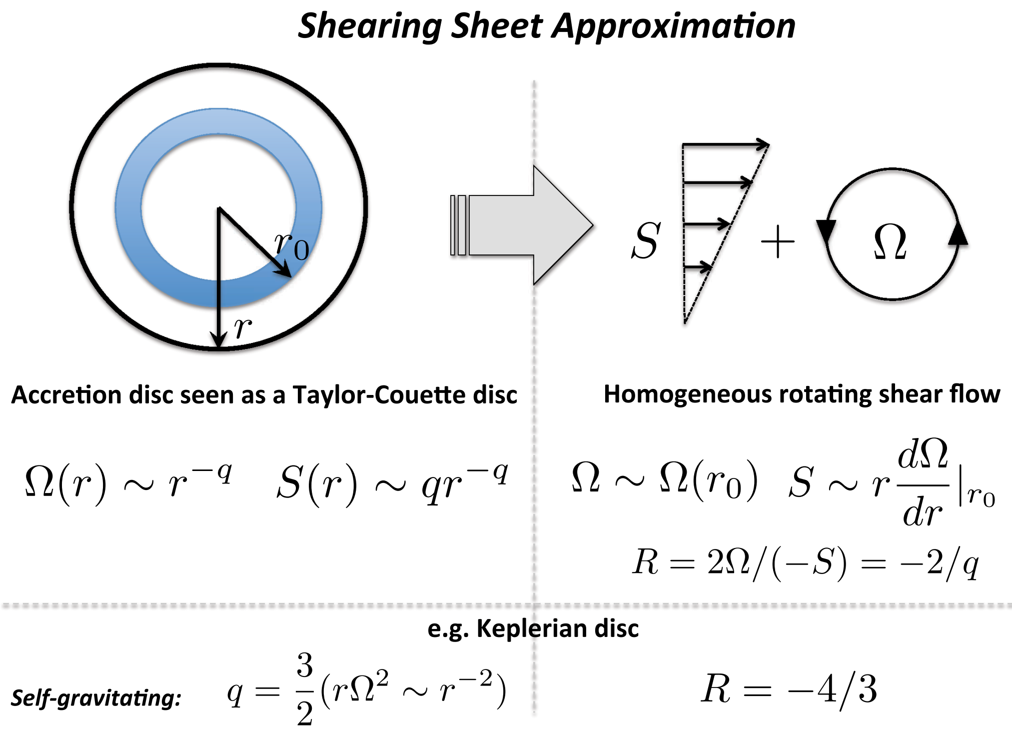

Figure 6. Scheme of the SSA for accretion discs.

other magnetized plasma discharges such as Hall-effect thrusters (Lafleur *et al.* [116], Koshkarov *et al.* [117], Charoy *et al.* [118]). This process is generally attributed to the turbulence that is driven by micro-instabilities. Historically, the Hasegawa–Mima equation and other reduced models were invoked to describe the oscillations of electric potential in tokamaks. In tokamaks, the interaction between disparate size structures such as zonal flows play an important role in both the regulation of plasma microturbulence and the full-scale dynamics (see Gürcan *et al.* [119] for a model of the turbulent spectra with disparate-scale interactions). Nowadays, turbulence is studied also in a kinetic framework, the phase space through the gyrokinetic description in theoretical models [120] or through the computational models such as GYSELA [121].

6. Conclusions on the future of CFD for fundamentals in fluid and MHD flows

In the present work, we have briefly reviewed the interplay and complementarity of CFD and theory in DNS and statistical theory approaches of turbulence. As seen in this work, significant progress has been made since the pioneering works in the 70s that were considering idealized flows (e.g., HIT in a periodic box) until the simulations of our days that involve additional body forces that introduce strong anisotropies, which are fundamental to fully understand turbulence in geophysical and astrophysical environments. As seen in Section 2.4, the Reynolds numbers that are achievable in DNS simulations are still limited nowadays by the computational costs. As stated by Chaouat [122], the computational time of a DNS simulation can be estimated to follow a law $t \propto Re^{11/4}$. This estimation shows that, despite the progress as predicted by Moore's law, DNS still remains difficult to avoid finite Reynolds effects (e.g., to capture decaying turbulence). Finally, other related topics that have not been treated in depth in this work but that are the result of the interaction between theory and CFD are the study of turbulence with complex geometries (of interest for different engineering applications), or the study of intermittency (see, e.g., Falkovich *et al.* [123] for a comprehensive review). Due to the complexity of these topics, further theoretical and numerical studies are still needed for a full understanding of these phenomena.

At the time of this writing, the installment of the first exascale supercomputer, Frontier, is already underway. Therefore, the comparative advantage is heavily favored by the CFD in solving idealized and practical turbulence problems. With the arrival of increasingly powerful supercomputers, the DNS would allow researchers to extract more complete sets of measurements concerning fully developed, complex turbulent flow fields far beyond those available from the statistical closure theories. Furthermore, the LES approach, which models the unresolvable scales with a statistical parameterization scheme, would give scientists access to much higher Reynolds number flows than those obtained from DNS. In some fundamental problems, where the order of magnitude of the dissipation rate is not known, as in astrophysics, the most convenient method is an ILES or a simple scheme of hyperviscosity. Taking advantage of the vast amount of data, turbulence theorists can play an important role in striving to further our understanding of the physics of turbulent flows, developing improved SGS models for LES or providing a more precise estimation of effective subgrid dissipation for ILES.

Theory, closures and beyond, and DNSs can cooperate in other domains. Theoretical studies of the infrared range can suggest "supergrid scale" models in a spectral zone where the resolution of DNSs is sparse, and especially its capture of directional anisotropy. About the spectral description, efforts will follow for unifying "weak" and "strong" turbulence. In this sense, we have emphasized multipoint spectral description, as "triads" for three-point triple correlations, especially with strong anisotropy and related elaborate numerics. This description is mandatory in wave turbulence theory, first for defining dispersion laws of waves, second for accounting for solenoidal (divergence-free in physical space) fields. For instance, the nonlinearity is cubic in plasma fields or in quantic turbulence, so that nonlinearity calls into play four-point fourth-order correlations, and therefore quartets in (solenoidal) Fourier space. This is the counterpart of triadic closures for quadratic nonlinearities, that were privilegied in our review. On the other hand, spectral description is only a mathematical convenience to treat both linear and nonlinear interactions of solenoidal fields. This is not an impediment to give results for statistical correlations in physical space, as for a possible extension of more anisotropic structure functions, that are more familiar for studying intermittency and scaling.

Conflicts of interest

Authors have no conflict of interest to declare.

Acknowledgements

The work of the third author was performed under the auspices of the Lawrence Livermore National Security, LLC under Contract No. DE-AC52-07NA27344.

References

[1] S. A. Orszag, G. S. Patterson, "Numerical simulation of three-dimensional homogeneous isotropic turbulence", *Phys. Rev. Lett.* **39** (1972), p. 76-79.

[2] Y. Zhou, "Turbulence theories and statistical closure approaches", *Phys. Rep.* **935** (2021), p. 1-117.

[3] M. Raffel, C. E. Willert, J. Kompenhans, *Particle Image Velocimetry: a Practical Guide*, vol. 2, Springer, Berlin, 1998.

[4] S. A. Orszag, "Analytical theories of turbulence", *J. Fluid Mech.* **41** (1970), p. 363-386.

[5] C. E. Leith, "Atmospheric predictability and two-dimensional turbulence", *J. Atmos. Sci.* **28** (1971), p. 145-161.

[6] P. K. Yeung, K. Ravikumar, "Advancing understanding of turbulence through extreme-scale computation: Intermittency and simulations at large problem sizes", *Phys. Rev. Fluids* **5** (2020), no. 11, article no. 110517.

[7] S. M. Ulam, *Adventures of a Mathematician*, University of California Press, Berkeley and Los Angeles, California, 1991.

[8] W. Aspray, *John von Neumann and the Origins of Modern Computing*, MIT Press, Cambridge, MA, 1990.

[9] P. Moin, K. Mahesh, "Direct numerical simulation: a tool in turbulence research", *Annu. Rev. Fluid Mech.* **30** (1998), no. 1, p. 539-578.

[10] D. Buaria, A. Pumir, E. Bodenschatz, P. K. Yeung, "Extreme velocity gradients in turbulent flows", *New J. Phys.* **21** (2019), article no. 043004.

[11] N. Cao, S. Chen, Z.-S. She, "Scalings and relative scalings in the Navier–Stokes turbulence", *Phys. Rev. Lett.* **76** (1996), p. 3711-3714.

[12] T. Ishihara, T. Gotoh, Y. Kaneda, "Study of high-Reynolds number isotropic turbulence by direct numerical simulation", *Annu. Rev. Fluid Mech.* **41** (2009), p. 165-180.

[13] K. P. Iyer, J. Schumacher, K. R. Sreenivasan, P. K. Yeung, "Steep cliffs and saturated exponents in three-dimensional scalar turbulence", *Phys. Rev. Lett.* **121** (2018), article no. 264501.

[14] K. P. Iyer, K. R. Sreenivasan, P. K. Yeung, "Circulation in high Reynolds number isotropic turbulence is a bifractal", *Phys. Rev. X* **9** (2019), article no. 041006.

[15] K. P. Iyer, K. R. Sreenivasan, P. K. Yeung, "Scaling exponents saturate in three-dimensional isotropic turbulence", *Phys. Rev. Fluids* **5** (2020), article no. 054605.

[16] Y. Kaneda, T. Ishihara, M. Yokokawa, K. I. Itakura, A. Uno, "Energy dissipation rate and energy spectrum in high resolution direct numerical simulations of turbulence in a periodic box", *Phys. Fluids* **15** (2003), p. L21-L24.

[17] P. K. Yeung, K. R. Sreenivasan, S. B. Pope, "Effects of finite spatial and temporal resolution in direct numerical simulations of incompressible isotropic turbulence", *Phys. Rev. Fluids* **3** (2018), article no. 064603.

[18] S. B. Pope, *Turbulent Flows*, Cambridge University Press, Cambridge, England, 2011.

[19] S. K. Lele, "Compact finite difference schemes with spectral-like resolution", *J. Comput. Phys.* **103** (1992), no. 1, p. 16-42.

[20] C. Hirsch, *Numerical Computation of Internal and External Flows*, vol. 2, Wiley, West Sussex, UK, 1990.

[21] J. P. Goedbloed, R. Keppens, S. Poedts, *Advanced Magnetohydrodynamics: With Applications to Laboratory and Astrophysical Plasmas*, Cambridge University Press, Cambridge, England, 2010.

[22] R. Rogallo, "Numerical experiments in homogeneous turbulence", 1981, NASA Tech. Mem. No. 81315.

[23] G. Lesur, P.-Y. Longaretti, "On the relevance of subcritical hydrodynamic turbulence to accretion disk transport", *Astron. Astrophys.* **444** (2005), p. 25-44.

[24] Y. Zhu, C. Cambon, F. S. Godeferd, A. Salhi, "Nonlinear spectral model for rotating sheared turbulence", *J. Fluid Mech.* **866** (2019), p. 5-32.

[25] V. Makarashvilia, E. Merzaria, A. Obabkoa, A. Siegela, P. Fischer, "A performance analysis of ensemble averaging for high fidelity turbulence simulations at the strong scaling limit", *Comput. Phys. Commun.* **219** (2017), p. 236-245.

[26] Y. Zhou, "Unification and extension of the similarity scaling criteria and mixing transition for studying astrophysics using high energy density laboratory experiments or numerical simulations", *Phys. Plasmas* **14** (2007), no. 8, article no. 082701.

[27] H. L. Grant, R. W. Stewart, A. Moilliet, "Turbulence spectra from a tidal channel", *J. Fluid Mech.* **12** (1962), no. 2, p. 241-268.

[28] A. A. Praskovsky, E. B. Gledzer, M. Y. Karyakin, Y. Zhou, "The sweeping decorrelation hypothesis and energy-inertial scale interaction in high Reynolds number flows", *J. Fluid Mech.* **248** (1993), p. 493-511.

[29] S. G. Saddoughi, S. V. Veeravalli, "Local isotropy in turbulent boundary layers at high Reynolds number", *J. Fluid Mech.* **268** (1994), p. 333-372.

[30] P. Sagaut, C. Cambon, *Homogeneous Turbulence Dynamics (Monograph)*, Springer, Cham, 2018.

[31] V. Bouillaut, S. Lepot, S. Aumaître, B. Gallet, "Transition to the ultimate regime in a radiatively driven convection experiment", *J. Fluid Mech.* **861** (2019), article no. R5.

[32] F. Waleffe, "The nature of triad interactions in homogeneous turbulence", *Phys. Fluids A* **4** (1992), p. 350-363.

[33] C. Cambon, L. Jacquin, "Spectral approach to non-isotropic turbulence subjected to rotation", *J. Fluid Mech.* **202** (1989), p. 295-317.

[34] F. Bellet, F. S. Godeferd, J. F. Scott, C. Cambon, "Wave-turbulence in rapidly rotating flows", *J. Fluid Mech.* **562** (2006), p. 83-121.

[35] S. Galtier, "Weak inertial wave-turbulence theory", *Phys. Rev. E* **68** (2003), article no. 015301.

[36] T. Le Reun, B. Gallet, B. Favier, M. Le Bar, "Near-resonant instability of geostrophic modes: beyond Greenspan's theorem", *J. Fluid Mech.* **900** (2020), article no. R2.

[37] Y. Zhou, “Rayleigh–Taylor and Richtmyer–Meshkov instability induced flow, turbulence, and mixing. I”, *Phys. Rep.* **720–722** (2017), p. 1-136.
[38] Y. Zhou, “Rayleigh–Taylor and Richtmyer–Meshkov instability induced flow, turbulence, and mixing. II”, *Phys. Rep.* **723–725** (2017), p. 1-160.
[39] Y. Zhou, T. T. Clark, D. S. Clark, S. Gail Glendinning, M. Aaron Skinner, C. M. Huntington, O. A. Hurricane, A. M. Dimits, B. A. Remington, “Turbulent mixing and transition criteria of flows induced by hydrodynamic instabilities”, *Phys. Plasmas* **26** (2019), no. 8, article no. 080901.
[40] Y. Zhou, R. J. Williams, P. Ramaprabhu, M. Groom, B. Thornber, A. Hillier, W. Mostert, B. Rollin, S. Balachandar, P. D. Powell, A. Mahalov, “Rayleigh–Taylor and Richtmyer–Meshkov instabilities: A journey through scales”, *Phys. D: Nonlinear Phenom.* **423** (2021), article no. 132838.
[41] O. Soulard, J. Griffond, B. J. Gréa, G. Viciconte, “Permanence of large eddies in decaying variable-density homogeneous turbulence with small Mach numbers”, *Phlys. Rev. Fluids* **5** (2020), no. 6, article no. 064613.
[42] A. Delache, C. Cambon, F. Godeferd, “Scale by scale anisotropy in freely decaying rotating turbulence”, *Phys. Fluids* **26** (2014), article no. 025104.
[43] R. Marino, P. D. Mininni, D. L. Rosenberg, A. Pouquet, “Large-scale anisotropy in stably stratified rotating flows”, *Phys. Rev. E* **90** (2014), article no. 023018.
[44] B. Galperin, S. Sukoriansky, “Turbulence in rotating fluids and the Nastrom and Gage spectrum”, in *Invited talk Sixth International Conference Turbulence Mixing and Beyond, ICTP, Trieste (Italy)*, 2017.
[45] B. Galperin, P. L. Read (eds.), *Zonal Jets: Phenomenology, Genesis, and Physics*, Cambridge University Press, Cambridge, England, 2019.
[46] B. McKeon, “The engine behind (wall) turbulence: Perspectives on scale interactions”, *J. Fluid Mech.* **817** (2017), article no. P1.
[47] B. F. Farrell, D. F. Gayme, P. J. Ioannou, “A statistical state dynamics approach to wall turbulence”, *Philos. Trans. R. Soc. A* **375** (2017), article no. 20160081.
[48] J. Smagorinsky, “General circulation experiments with the primitive equations: I. The basic experiment”, *Mon. Weather Rev.* **91** (1963), p. 99-164.
[49] G. Holloway, “Entropic forces in geophysical fluid dynamics”, *Entropy* **11** (2009), no. 3, p. 360-383.
[50] J. A. van Hooft, S. Popinet, B. J. H. van de Wiel, “Adaptive Cartesian meshes for atmospheric single-column models: a study using Basilisk 18-02-16”, *Geosci. Model Dev.* **11** (2018), p. 4727-4738.
[51] P. Gent, J. C. McWilliams, “Isopycnal mixing in ocean circulation models”, *J. Phys. Oceanogr.* **20** (1990), no. 1, p. 150-155.
[52] P. D. Williams, “Increased light, moderate, and severe clear-air turbulence in response to climate change”, *Adv. Atmos. Sci.* **34** (2017), p. 576-586.
[53] S. Watanabe, M. Fujita, S. Kawazoe, S. Sugimoto, Y. Okada, R. Mizuta, M. Ishii, “Frequency change of clear-air turbulence over the north Pacific under 2 k global warming—ensemble projections using a 60-km atmospheric general circulation model”, *J. Meteorol. Soc. Jpn Ser II* **97** (2019), p. 757-771.
[54] M. Ghil, V. Lucarini, “The physics of climate variability and climate change”, *Rev. Mod. Phys.* **92** (2020), article no. 035002.
[55] K. G. Pressel, S. Mishra, T. Schneider, C. M. Kaul, Z. Tan, “Numerics and subgrid-scale modeling in large eddy simulations of stratocumulus clouds”, *J. Adv. Model. Earth Syst.* **9** (2017), p. 1342-1365.
[56] D. Biskamp, *Magnetohydrodynamic Turbulence (Monograph)*, Cambridge University Press, Cambridge, England, 2003.
[57] A. Schekochihin, “MHD turbulence: A biased review”, *J. Plasma Phys.* **88** (2022), no. 5, article no. 155880501.
[58] Y. Zhou, W. H. Matthaeus, P. Dmitruk, “Colloquium: Magnetohydrodynamic turbulence and time scales in astrophysical and space plasmas”, *Rev. Mod. Phys.* **76** (2004), no. 4, p. 1015-1035.
[59] K. H. Kiyani, K. T. Osman, S. C. Chapman, “Dissipation and heating in solar wind turbulence: from the macro to the micro and back again”, *Philos. Trans. R. Soc. A* **373** (2015), article no. 20140155.
[60] P. Goldreich, S. Sridhar, “Toward a theory of interstellar turbulence. 2: Strong Alfvenic turbulence”, *Astrophys. J.* **438** (1995), p. 763-775.
[61] D. Fyfe, D. Montgomery, G. Joyce, “Magnetic dynamo action in two-dimensional turbulent magneto-hydrodynamics”, *J. Plasma Phys.* **17** (1977), p. 317-335.
[62] A. Pouquet, G. Patterson, “Numerical simulation of helical magnetohydrodynamic turbulence”, *J. Fluid Mech.* **85** (1978), no. 2, p. 305-323.
[63] S. A. Orszag, C. M. Tang, “Small-scale structure of two-dimensional magnetohydrodynamic turbulence”, *J. Fluid Mech.* **90** (1979), p. 129-143.
[64] D. Biskamp, H. Welter, “Dynamics of decaying two-dimensional magnetohydrodynamics turbulence”, *Phys. Fluids B* **1** (1989), p. 1964-1979.
[65] H. Politano, A. Pouquet, P. L. Sulem, “Current and vorticity dynamics in three-dimensional magnetohydrodynamic turbulence”, *Phys. Plasmas* **2** (1995), p. 2931-2939.

[66] D. Biskamp, W.-C. Muller, "Decay laws for three-dimensional magnetohydrodynamic turbulence", *Phys. Rev. Lett.* **83** (1999), p. 2195-2198.

[67] P. D. Mininni, A. Pouquet, "Energy spectra stemming from interactions of Alfvén waves and turbulent eddies", *Phys. Rev. Lett.* **99** (2007), article no. 254502.

[68] S. Boldyrev, "Spectrum of magnetohydrodynamic turbulence", *Phys. Rev. Lett.* **96** (2006), article no. 115002.

[69] A. Beresnyak, "The spectral slope and Kolmogorov constant of MHD turbulence", *Phys. Rev. Lett.* **106** (2011), article no. 075001.

[70] A. Beresnyak, "Spectra of strong magnetohydrodynamic turbulence from high-resolution simulations", *Astrophys. J.* **784** (2014), article no. L20.

[71] M. Linkmann, A. Berera, E. E. Goldstraw, "Reynolds-number dependence of the dimensionless dissipation rate in homogeneous magnetohydrodynamic turbulence", *Phys. Rev. E* **95** (2017), no. 1, article no. 013102.

[72] R. Bandyopadhyay, S. Oughton, M. Wan, W. H. Matthaeus, R. Chhiber, T. N. Parashar, "Finite dissipation in anisotropic magnetohydrodynamic turbulence", *Phys. Rev. X* **8** (2018), no. 4, article no. 041052.

[73] X. M. Zhai, K. R. Sreenivasan, P. K. Yeung, "Cancellation exponents in isotropic turbulence and magnetohydrodynamic turbulence", *Phys. Rev. E* **99** (2019), no. 2, article no. 023102.

[74] X. M. Zhai, P. K. Yeung, "Evolution of anisotropy in direct numerical simulations of MHD turbulence in a strong magnetic field on elongated periodic domains", *Phys. Rev. Fluids* **3** (2018), article no. 084602.

[75] V. E. Zakharov, V. S. L'vov, G. Falkovich, *Kolmogorov Spectra of Turbulence I: Wave Turbulence*, Springer, Berlin, 1992.

[76] S. Nazarenko, *Wave Turbulence*, Springer, Berlin, 2011.

[77] S. Galtier, S. V. Nazarenko, A. C. Newell, A. Pouquet, "A weak turbulence theory for incompressible magnetohydrodynamics", *J. Plasma Phys.* **63** (2000), p. 447-448.

[78] C. Cambon, R. Rubinstein, F. S. Godeferd, "Advances in wave turbulence: Rapidly rotating flows", *New J. Phys.* **6** (2004), article no. 73.

[79] A. Pouquet, U. Frisch, J. Leorat, "Strong MHD helical turbulence and the nonlinear dynamo effect", *J. Fluid Mech.* **77** (1976), p. 321-354.

[80] W. H. Matthaeus, Y. Zhou, "Extended inertial range phenomenology of magnetohydrodynamic turbulence", *Phys. Fluids B* **1** (1989), p. 1929-1931.

[81] R. Grappin, U. Frisch, A. Pouquet, J. Leorat, "Alfvnic fluctuations as asymptotic states of MHD turbulence", *Astron. Astrophys.* **105** (1982), p. 6-14.

[82] R. Grappin, J. Leorat, A. Pouquet, "Dependence of MHD turbulence spectra on the velocity field-magnetic field correlation", *Astron. Astrophys.* **126** (1983), p. 51-58.

[83] A. Briard, T. Gomez, "The decay of isotropic magnetohydrodynamics turbulence and the effects of cross-helicity", *J. Plasma Phys.* **84** (2018), article no. 905840110.

[84] C. Cambon, "Homogeneous MHD turbulence at weak magnetic Reynolds numbers: approach to angular-dependent spectra", in *Advances in Turbulence Studies* (H. Branover, Y. Unger, eds.), Progresses in Astronautics and Aeronautics, vol. 149, AIAA, Washington, DC, 1991, ISBN 1-56347-018-7, p. 131-145.

[85] B. F. N. Favier, F. S. Godeferd, C. Cambon, "On the effect of rotation on magnetohydrodynamic turbulence at high magnetic Reynolds number", *Geophys. Astrophys. Fluid Dyn.* **106** (2011), p. 89-111.

[86] Y. Zhou, W. H. Matthaeus, "Phenomenology treatment of magnetohydrodynamic turbulence with nonequipartition and anisotropy", *Phys. Plasmas* **12** (2005), article no. 056503.

[87] C. S. Ng, A. Bhattacharjee, "Scaling of anisotropic spectra due to the weak interaction of shear-Alfvén wave packets", *Phys. Plasmas* **4** (1997), p. 605-610.

[88] M. Miesch, W. Matthaeus, A. Brandenburg, A. Petrosyan, A. Pouquet, C. Cambon, F. Jenko, D. Uzdensky, J. Stone, S. Tobias, J. Toomre, "Large-eddy simulations of magnetohydrodynamic turbulence in heliophysics and astrophysics", *Space Sci. Rev.* **194** (2015), p. 97-137.

[89] O. Agullo, W. C. Müller, B. Knaepen, D. Carati, "Large eddy simulation of decaying magnetohydrodynamic turbulence with dynamic subgrid-modeling", *Phys. Plasmas* **8** (2001), p. 3502-3505.

[90] W. C. Müller, D. Carati, "Dynamic gradient-diffusion subgrid models for incompressible magnetohydrodynamic turbulence", *Phys. Plasmas* **9** (2002), p. 824-834.

[91] B. Knaepen, P. Moin, "Large-eddy simulation of conductive flows at low magnetic Reynolds number", *Phys. Fluids* **16** (2004), p. 1255-1261.

[92] A. Yoshizawa, "Subgrid modeling for magnetohydrodynamic turbulent shear flows", *Phys. Fluids* **30** (1987), p. 1089-1095.

[93] Y. Zhou, O. Schilling, S. Ghosh, "Subgrid scale and backscatter model for magnetohydrodynamic turbulence based on closure theory: Theoretical formulation", *Phys. Rev. E* **66** (2002), article no. 026309.

[94] H. Aluie, "Coarse-grained incompressible magnetohydrodynamics: Analyzing the turbulent cascades", *New J. Phys.* **19** (2017), article no. 025008.

[95] Y. Zhou, "Renormalization group theory for fluid and plasma turbulence", *Phys. Rep.* **488** (2010), p. 1-9.

[96] D. H. Hathaway, "The solar cycle", *Living Rev. Sol. Phys.* **12** (2015), article no. 4.

[97] P. Chabonneau, "Dynamo models of the solar cycle", *Living Rev. Sol. Phys.* **17** (2020), article no. 4.
[98] S. Lantz, Y. Fan, "Anelastic magnetohydrodynamic equations for modeling solar and stellar convection zones", *Astrophys. J. Suppl. Ser.* **121** (1999), p. 247-264.
[99] S. I. Braginsky, P. H. Roberts, "Equations governing convection in earth's core and the geodynamo", *Geophys. Astrophys. Fluid Dyn.* **79** (1995), no. 1–4, p. 1-97.
[100] Y. Zhou, F. F. Grinstein, A. J. Wachtor, B. M. Haines, "Estimating the effective Reynolds number in implicit large-eddy simulation", *Phys. Rev. E* **89** (2014), article no. 013303.
[101] A. S. Brun, M. S. Miesch, J. Toomre, "Global-scale turbulent convection and magnetic dynamo action in the solar envelope", *Astrophys. J.* **614** (2004), p. 1073-1098.
[102] I. N. Kitiashvili, A. G. Kosovichev, N. N. Mansour, A. A. Wray, "Realistic modeling of local dynamo processes on the Sun", *Astrophys. J.* **809** (2015), no. 1, article no. 84.
[103] A. A. Wray, K. Bensassi, I. N. Kitiashvili, N. N. Mansour, A. G. Kosovichev, "Simulations of stellar magnetoconvection using the radiative MHD code 'StellarBox'", 2015, ArXiv e-prints, https://arxiv.org/abs/1507.07999.
[104] P. Moin, K. Squires, W. Cabot, S. Lee, "A dynamic subgrid-scale model for compressible turbulence and scalar transport", *Phys. Fluids A: Fluid Dyn.* **3** (1991), no. 11, p. 2746-2757.
[105] A. Alvarez Laguna, *Multi-fluid modeling of magnetic reconnection in solar partially ionized and laboratory plasmas*, PhD Thesis, VKI, 2018.
[106] A. Alvarez Laguna, A. Lani, N. N. Mansour, H. Deconinck, S. Poedts, "Effect of radiation on chromospheric magnetic reconnection: reactive and collisional multi-fluid simulations", *Astrophys. J.* **842** (2017), article no. 117.
[107] E. Khomenko, M. Collados, T. Felipe, "Nonlinear numerical simulations of magneto-acoustic wave propagation in small-scale flux tubes", *Solar Phys.* **251** (2008), p. 589-611.
[108] Y. G. Maneva, A. A. Laguna, A. Lani, S. Poedts, "Multi-fluid modeling of magnetosonic wave propagation in the solar chromosphere: effects of impact ionization and radiative recombination", *Astrophys. J.* **836** (2017), no. 2, article no. 197.
[109] B. V. Gudiksen, M. Carlsson, V. H. Hansteen, W. Hayek, J. Leenaarts, J. Martnez-Sykora, "The stellar atmosphere simulation code Bifrost", *Astron. Astrophys.* **531** (2011), article no. A154.
[110] I. Kitiashvili, A. Wray, V. Sadykov, A. Kosovichev, N. Mansour, "Realistic 3D MHD modeling of self-organized magnetic structuring of the solar corona", *Proc. Int. Astron. Union* **15** (2019), no. S354, p. 346-350.
[111] B. van der Holst, I. V. Sokolov, X. Meng, M. Jin, W. B. Manchester IV, G. Tóth, T. I. Gombosi, "Alfvén wave solar model (AWSoM): coronal heating", *Astrophys. J.* **782** (2014), p. 81-96.
[112] P. Dmitruk, W. H. Matthaeus, L. J. Milano, S. Oughton, G. P. Zank, D. J. Mullan, "Coronal heating distribution due to low-frequency, wave-driven turbulence", *Astrophys. J.* **575** (2002), p. 571-577.
[113] S. A. Balbus, J. F. Hawley, "A powerful local shear instability in weakly magnetized discs", *Astrophys. J.* **376** (1991), p. 214-233.
[114] A. Salhi, C. Cambon, "An analysis of rotating shear flow using linear theory and DNS and LES results", *J. Fluid Mech.* **347** (1997), p. 171-195.
[115] R. Balescu, *Aspects of Anomalous Transport in Plasmas*, CRC Press, Bristol, UK, 2005.
[116] T. Lafleur, S. D. Baalrud, P. Chabert, "Characteristics and transport effects of the electron drift instability in Hall-effect thrusters", *Plasma Sources Sci. Technol.* **26** (2017), article no. 024008.
[117] O. Koshkarov, A. Smolyakov, Y. Raitses, I. Kaganovich, "Self-organization, structures, and anomalous transport in turbulent partially magnetized plasmas with crossed electric and magnetic fields", *Phys. Rev. Lett.* **122** (2019), article no. 185001.
[118] T. Charoy, T. Lafleur, A. Alvarez-Laguna, A. Bourdon, P. Chabert, "The interaction between ion transit-time and electron drift instabilities and their effect on anomalous electron transport in Hall thrusters", *Sources Sci. Technol.* **30** (2021), article no. 065017.
[119] O. D. Gürkan, X. Garbet, P. Hennequin, P. H. Diamond, A. Casati, G. L. Falchetto, "Wave-number spectrum of drift-wave turbulence", *Phys. Rev. Lett.* **102** (2009), no. 25, article no. 255002.
[120] A. A. Schekochihin, S. C. Cowley, W. Dorland, G. W. Hammett, G. G. Howes, G. G. Plunk, E. Quataert, T. Tatsuno, "Gyrokinetic turbulence: a nonlinear route to dissipation through phase space", *Plasma Phys. Control. Fusion* **50** (2008), no. 12, article no. 124024.
[121] V. Grandgirard, Y. Sarazin, X. Garbet, G. Dif-Pradalier, P. Ghendrih, N. Crouseilles, G. Latu, E. Sonnendrücker, N. Besse, P. Bertrand, "GYSELA, a full-f global gyrokinetic semi-Lagrangian code for ITG turbulence simulations", *AIP Conf. Proc.* **871** (2006), no. 1, p. 100-111.
[122] B. Chaouat, "The state of the art of hybrid RANS/LES modeling for the simulation of turbulent flows", *Flow Turbul. Combust.* **99** (2017), p. 279-327.
[123] G. Falkovich, K. Gawedzki, M. Vergassola, "Particles and fields in fluid turbulence", *Rev. Mod. Phys.* **73** (2001), p. 913-975.